NASA TECHNICAL NOTE

NASA TN D-3012

CALORIMETRIC EVALUATION OF A 60-INCH (152-CENTIMETER) ELECTROFORMED NICKEL SOLAR CONCENTRATOR

by Conrad M. Willis

Langley Research Center
Langley Station, Hampton, Va.

NATIONAL AERONAUTICS AND SPACE ADMINISTRATION • WASHINGTON, D. C. • SEPTEMBER 1965

CALORIMETRIC EVALUATION OF A 60-INCH (152-CENTIMETER) ELECTROFORMED NICKEL SOLAR CONCENTRATOR

By Conrad M. Willis

Langley Research Center
Langley Station, Hampton, Va.

NATIONAL AERONAUTICS AND SPACE ADMINISTRATION

For sale by the Clearinghouse for Federal Scientific and Technical Information
Springfield, Virginia 22151 – Price $1.00

CALORIMETRIC EVALUATION OF A 60-INCH (152-CENTIMETER) ELECTROFORMED NICKEL SOLAR CONCENTRATOR

By Conrad M. Willis
Langley Research Center

SUMMARY

Concentrator efficiency over a range of absorber aperture sizes has been determined for a paraboloidal solar concentrator. The concentrator was a 60° rim angle, 60-inch (152-cm) electroformed-nickel model considered suitable for use in space-vehicle power-generation systems. Tests were conducted with the concentrator mounted on a solar tracker with a water-cooled cavity calorimeter used as the heat absorber. A concentrating efficiency of 0.75 was measured at a concentration ratio of 13,300. Misorientation tests indicated small errors in lateral location of the calorimeter could be compensated by angular adjustment of the concentrator axis with respect to the sun.

INTRODUCTION

Solar concentrators show considerable promise as a means of supplying power for space vehicles. (See refs. 1 and 2.) Some of the results of research and development programs on various types of concentrators and conversion devices are discussed in references 3 to 6.

This paper presents the results of solar tests of a one-piece, 60-in. (152-cm) diameter, paraboloidal solar concentrator. A cold calorimeter (one operating at near ambient temperatures to reduce reradiation) was used as a heat receiver. As the reradiation from the calorimeter was negligible, the calorimetric efficiencies reported herein are a measure of the reflectance and concentrating ability of the concentrator alone and are not a measure of the efficiency of a complete power system. Since higher cavity temperatures are required for efficient converter operation, the reradiation losses increase and the energy available for conversion will be less than that indicated by the cold calorimeter tests. In an actual power system, the cavity aperture diameter must be kept small enough to reduce the reradiation losses and to attain the operating temperature of the selected type of conversion device; at the same time this aperture must be large enough to attain good calorimetric efficiency. Therefore, the optimum aperture size will depend upon both converter type and concentrator quality. The test concentrator was designed to have an accuracy suitable for use with thermionic conversion devices, or cavity temperatures of 1600° K to 2100° K (ref. 6). Concentrator efficiency was determined for an

aperture diameter range of 0.500 to 2.000 inches (1.270 to 5.080 cm); such a range would include optimum diameters for thermionic converter operation.

SYMBOLS

The units used for the physical quantities defined in this paper are given in both the U.S. Customary Units and in the International System of Units (SI) (ref. 7). An appendix is included for the purpose of explaining the relationships between these two systems of units.

A	unobscured projected area of concentrator or total projected area of reflective surface minus area shaded by calorimeter and supports, ft^2 (m^2)
C	concentration ratio, ratio of projected unobscured concentrator area to calorimeter aperture area, $\frac{A}{\pi r^2}$
D	concentrator diameter, in. (cm)
f	focal-length setting, measured distance along optical axis from concentrator vertex to calorimeter aperture, in. (cm)
k	constant for calculating η (17.57 in U.S. Customary units; 4,183 in SI units)
r	radius of calorimeter aperture, in. (cm)
ΔT	temperature increase of water flowing through calorimeter, F^o (K^o)
w	mass flow rate of calorimeter water, lbm/min (kg/s)
x	distance from paraboloid axis to center of calorimeter aperture, measured along either of two orthogonal axes, in. (cm)
β	misorientation angle, angle between paraboloid axis and solar rays, minutes
γ	solar constant or rate of energy falling on a unit area lying perpendicular to solar rays, watts/ft^2 (watts/m^2)
η	calorimetric efficiency, ratio of energy absorbed by calorimeter water to energy incident on the concentrator, $\frac{kw\Delta T}{\gamma A}$

APPARATUS AND MODEL

Apparatus.- A modified military searchlight chassis was used as a solar tracking system. A schematic drawing of the tracker is shown in figure 1 and photographs of the tracker and equipment are shown in figures 2 and 3. The solar concentrator was mounted on the tracker and the tracker was rotated automatically about azimuth and elevation axes to maintain any set orientation with the sun. The tracking sensor used consisted of a tube having a radiation-sensitive transducer mounted at one end and an aperture for admitting a narrow beam of sunlight in the opposite end. An error signal was generated when the beam of light moved away from the transducer center and servomotors rotated the tracker until the light beam was recentered. A 32× tracking-error telescope (fig. 1) projected the sun's image on to an error screen inscribed with concentric circles indicating various amounts of misorientation. Tracking accuracy, as measured by the screen, was ±0.3 minute. The error screen was also used to measure small misorientation angles during off-axis testing. The intensity of the incident solar radiation was measured by a normal-incidence pyrheliometer.

A schematic diagram of the test facility is shown in figure 4. A steady rate of water flow was maintained through the calorimeter by using an elevated, continuously overflowing supply tank. The calorimeter (figs. 5 and 6) consisted of a cylindrical cavity and a set of interchangeable aperture plates. Aperture diameter ranged from 0.37 inch to 2.00 inches (0.94 cm to 5.08 cm) to allow testing over a range of concentration ratios. The cavity was formed of a helical winding of copper tubing and was coated with carbon black to increase absorptivity. A layer of foamed-in-place plastic insulated the copper tubing from the outside case. A sheathed copper-constantan thermocouple junction measured the inlet temperature of the calorimeter water. Two other junctions were connected to measure the temperature differential between inlet and outlet. A separate water circuit provided aperture plate cooling to carry away energy falling outside the aperture.

The calorimeter could be moved along three orthogonal axes by adjusting screws. The range of calorimeter travel was about 2 inches (5 cm) along the optical axis and 1 inch (3 cm) along the two axes perpendicular to the optical axis. An obscurant disk (fig. 1) masked the concentrator vertex to maintain a fixed reflective surface for all calorimeter locations.

Wind screens were erected and counterweights hung on the tracker to reduce concentrator vibration on windy days. Recording potentiometers were used to read out the thermocouples and pyrheliometer. Water flow rate was measured by a glass tube and float type of meter. A turbine type of flowmeter with an impulse counter and timer readout was used to make occasional checks on the float meter.

Model.- The concentrator model consisted of a reflective paraboloidal shell with a rim-mounted supporting torus. Dimensions and some of the construction details are shown in figure 7. Nominal design values were a rim angle of 60° and a diameter of 60 inches (152 cm) which give a calculated focal length of 25.98 inches (65.99 cm). The concentrator mass was 17.5 lbm (7.9 kg). The paraboloidal electroformed nickel shell was joined to the aluminum torus with a

cylindrical nickel skirt. The shell-skirt and the skirt-torus joints were made by secondary electroforming. Figure 8(a) is a partial rear view of the concentrator that shows the joining of the torus and the cylindrical skirt. Also shown is one of the three tapped inserts in the torus that were used as concentrator mounting points. The paraboloidal shell was electroformed on a glass searchlight reflector and was subsequently coated with a vacuum-deposited aluminum reflective layer. The aluminum coating did not adhere to a long narrow roughened area (fig. 8(b) corresponding to a crack in the glass searchlight master. The loss in reflective surface was about 0.3 percent of the concentrator projected area. The central hole in the concentrator was shaded by the calorimeter during tests and did not reduce the effective area of the concentrator. Further details on electroformed concentrator construction are given in reference 8.

TESTS

The concentrator was alined roughly by centering on the tracker mounting bars. A discrete Hartmann screen (fig. 3) was then mounted in front of the concentrator. This screen was made of sheet metal and was slightly larger than the concentrator. Four radial rows of 0.25-inch (0.64-cm) holes were drilled in the screen and each hole was equipped with an individual cover. With the tracker following the sun, 4 holes spaced 90° apart and equally distant from the center were uncovered to allow sunlight to pass through the holes and to be reflected from the concentrator to an image plate. A spacing of about 1 inch (3 cm) between images was obtained by axial movement of the image plate. A symmetrical image pattern (fig. 9), indicating alinement of the optical axis with the solar rays, was obtained and located near the center of the plate by moving the concentrator on its mounts. The screen was then rotated and the changing image-pattern observed for symmetry. Patterns at other radii were observed and the concentrator mounting bolts locked at the estimated best position. Final centering of the image pattern was obtained by moving the image plate and/or by adjusting the orientation of the tracking sensor.

For the next part of the test, the Hartmann screen was replaced by an aluminized plastic filter which attenuated the solar energy enough to prevent melting of the image plate when the solar image produced by the entire concentrator was examined. Observation of image size, symmetry, and sharpness gave some indication of concentrator quality. Some improvement in image symmetry was obtained by varying the torque applied in tightening the concentrator mounting bolts. Alinement and mounting of the concentrator were now considered to be satisfactory, and the calorimeter was placed at the former location of the image plate.

During calorimetric testing the calorimeter was moved along the three orthogonal axes, one of which was the concentrator optical axis. The orientation of the optical axis with respect to the sun was also varied to determine the maximum efficiency obtainable and the penalties incurred by misalinement. The first focal region search consisted of moving the calorimeter along the concentrator axis in small steps while observing the water ΔT to locate the focal length producing a maximum efficiency. The calorimeter was next moved along the

two axes perpendicular to the optical axis to determine the best lateral location. After the best lateral position was located, the optimum focal length was checked again and the distance from aperture to mirror was measured. The focal-length settings made during testing were measured to a reference position on the calorimeter mount for convenience and accuracy. The first searches were made with a 0.500-inch-diameter (1.27-cm) aperture which is approximately the same size as the maximum intensity portion of the image, and thus produced maximum sensitivity in locating the focal point.

In addition to searches in which x, f, and β were varied individually, a search with combined location and orientation errors was made to obtain data for the case of simultaneous occurrence of more than one type of error.

Test variables and ambient conditions ranged as follows: aperture sizes of 0.375 to 2.000 inches (0.950 to 5.080 centimeters) corresponding to concentration ratios of 24,000 to 830; misorientation angles of ±50 minutes; calorimeter water-flow rates of 1.25 to 1.42 lbm/min (9.45 to 10.74 g/s); water temperature differential from inlet to outlet of 10 F° to 60 F° (6 K° to 33 K°); with water inlet temperatures of 40° F to 90° F (277.3° K to 305.0° K); ambient air temperatures of 25° F to 95° F (269° K to 308° K); and solar-radiation intensities of 58 to 90 watts per square foot (620 to 970 w/m^2). Additional discussion of test apparatus and techniques for solar concentrator evaluation can be found in reference 8.

ACCURACY OF DATA

The temperature-compensated pyrheliometer was factory calibrated and was also calibrated against an instrument which had been checked with a Smithsonian Institution standard. The mean difference between readings of the reference instrument and the test pyrheliometer was 0.3 percent. The manufacturer of the potentiometer used to measure pyrheliometer output, quoted an accuracy of 0.25 percent of the full-scale reading or 0.7 percent for the test range measured.

Manufacturer's calibrations of the thermocouples indicate that deviations from the National Bureau of Standards tables were negligible. Accuracy of the readout potentiometer for ΔT was 0.5 percent of full-scale or 1.2 percent of the average test value.

The flowmeter was calibrated by weighing the water delivered in a timed interval. Based on repeatability of readings, the standard deviation was ±0.4 percent. A calorimeter calibration to determine the amount of heat conducted through the walls was obtained by running hot water through the calorimeter and measuring the temperature drop. The calibration data were used to calculate the thermal conductivity of the calorimeter at the flow rates used during testing. This experimentally determined conductivity was then used to calculate the heat transfer through the walls for the most extreme conditions of these tests. With a high calorimeter input (largest aperture and clear day) and cold ambient air, the loss would be 0.5 percent. With a low input (smallest aperture, hazy day) and high temperature, the calorimeter case might become

hotter than the outlet water temperature and produce gains in efficiency of 0.5 percent. The potentiometer errors and calorimeter losses listed were considered to represent three standard deviations for the calculation of probable error. A probable error of 0.14 percent was assigned to the measurement of concentrator area. The calculated probable error in calorimetric efficiency is 0.0035 for the individual errors previously listed. This error amounts to a probable error of about ±0.5 percent for calorimetric efficiencies near 0.75 and is in good agreement with the repeatability of data obtained on successive days.

RESULTS AND DISCUSSION

A thorough calorimetric exploration of the concentrator focal region was carried out, primarily to determine the aperture location producing the highest efficiency. The concentrator focal point is then considered to be located at the center of the aperture. Additional information such as image size and flux distribution may be deduced from the data.

As was previously noted, the cursory search along the concentrator axis established a tentative focal length, and then the transverse searches were made. Figure 10 shows the variation in calorimetric efficiency with transverse (lateral) movement of the calorimeter. Data obtained by separate searches along the two axes were combined in this figure. The zero location for lateral movements of the calorimeter was determined experimentally by plotting the data for one of the smaller apertures and selecting the location producing maximum efficiency. All lateral measurements were then referenced to this selected location. It should be realized, however, that the selected best focal point of the concentrator does not necessarily lie on the geometrical axis of the nominal perfect paraboloid. Any nonsymmetrical distortions of the reflective surface incurred during fabrication and mounting will move the optical axis with respect to its design position. Also, the optical axis movement may be increased by any small pointing errors made in alining the concentrator with the solar rays. Note in figure 10 that the curves for the larger apertures are flat, whereas the aperture sizes near the 0.6-inch (1.5-cm) theoretical image size show a sharp drop in efficiency for small aperture mislocations. This sharp drop indicates an image size that is not much larger than that for a perfect paraboloid. The flatness of the curve for the 1.25-inch (3.17-cm) aperture indicates that the image was almost completely enclosed throughout the lateral range of the tests.

The variation in concentrator calorimetric efficiency as a function of aperture location along the optical axis is shown in figure 11. It can be seen from the figure that the highest efficiency or best focus occurs near an f/D value of about 0.427. The minor variations from this value may be due to some combination of experimental error and focal-image distortion due to concentrator surface error. However, the variation is not considered to be significant. The nominal values given for diameter and focal length in the manufacturer's description of the master result in a f/D ratio of 0.433, or about $1\frac{1}{2}$ percent larger than measured. The reason for the difference between master and copy is not known. However, this difference is not considered to be important because a heat receiver location would be based on the measured concentrator focal length.

The maximum calorimetric efficiency obtained with each aperture during the various focal region searches is presented as a function of concentration ratio in figure 12. At the lower concentration ratios or larger aperture sizes, the flatness of the curve indicates that nearly all the specularly reflected energy is entering the calorimeter. Since calorimeter reradiation losses were small at the test temperatures, the maximum concentrating efficiency is therefore approximately equal to concentrator specular reflectance. Maximum efficiency for this concentrator was about 0.86. At a concentration ratio of 13,300, which would provide temperatures high enough to be suitable for use in a thermionic conversion system, a concentrating efficiency of 0.75 was obtained.

Also included in figure 12 are some data from reference 9 representing the state of the art for electroformed concentrators. Both concentrators were electroformed over the same master and were the seventh and sixteenth models replicated. The master crack, reproduced in the present model (fig. 8(b)), occurred sometime between the fabrication of the two concentrators. Efficiencies for the reference concentrator are about 0.02 higher at the largest apertures tested and about 0.10 higher at a concentration ratio of 13,300. Some of the 0.02 loss is due to a bond failure of the reflective coating in the crack area. However, the area affected by the crack was only 0.3 percent of the total. The remainder of the 0.02 difference is attributed to degradation during storage and to the accuracies with which the two sets of data were obtained.

An attempt was made to explain the 0.10 difference in efficiencies at high concentration ratios on the basis of concentrator distortion adjacent to the support torus. The concentrator of reference 9 had an overall diameter of 66 inches (168 cm) and an annular mask was used to reduce the effective diameter to 60 inches (152 cm). Since some rim distortion had been observed both visually and by optical tests during the present investigation, a mask was made to shade the rim area. A reduction in projected area of about 11.5 percent reduced the heat input to the calorimeter about 4.3 percent or increased the efficiency about 0.056. Note that some of this increase is produced by the smaller image size at the new effective rim angle. Since this increase is less than the 0.10 difference in the two concentrator efficiencies, there is apparently some real difference because of surface slope errors in addition to the difference due to test techniques.

An indication of the pointing accuracy required is shown in figure 13 where calorimetric efficiency is presented as a function of the angle between the solar rays and the concentrator optical axis. For a concentration ratio of 13,300, a loss in concentrating efficiency of 0.10 occurs with a misorientation of about 12 minutes. For larger apertures the central part of the curve is flatter and for a concentration ratio of 830, a misorientation of about 50 minutes is required to produce the same loss in efficiency. This characteristic flattening of the efficiency curve indicates that orientation requirements can be less stringent for conversion systems using relatively large apertures. However, it should be noted that the drop-off in efficiency becomes sharp for all orifice sizes when the misorientation becomes large enough for part of the image to fall outside the aperture boundary. The curve asymmetry is believed to be due to imperfect concentrator geometry.

The effects of lateral displacement of the heat absorber and angular orientation of the concentrator optical axis have been shown in figures 10 and 13, respectively. Concentrator efficiency with combined errors consisting of concentrator misorientation and both lateral and axial mislocations of the calorimeter are presented in figure 14. It is reasonable to assume that a small concentrator misorientation produces corresponding small changes in image size and shape, the main change being in image location. Therefore, small errors in either concentrator orientation or calorimeter location can be nearly compensated by adjustment of the other. The orientation searches at a number of lateral aperture locations (fig. 14) provide experimental verification of this assumption. A comparison of the peak efficiencies for the same focal length throughout the range of x-settings shows that the efficiencies are approximately equal and vary less than ± 0.01. Thus, when values are read for the on-focus peaks of figure 14 at $x/D = -0.00078$ and 0.00208, the $x/D = 0.00286$ lateral movement of the calorimeter is compensated by a 14-minute change in orientation of the concentrator-calorimeter system with respect to the sun. Therefore, if flight hardware for this type of system has a means for adjusting the orientation of the tracking sensor, small lateral errors occurring during deployment can be compensated for without the additional complexity of a lateral adjusting mechanism.

The efficiency data shown in figure 14 were taken late in the test program and are about 0.03 lower than previously shown (fig. 11) for a concentration ratio of 13,300. This loss is believed to be due to a gradual deterioration of the reflective surface. The reflective coating of vacuum-deposited aluminum did not have a protective overcoat and had been washed twice before these data were obtained.

CONCLUDING REMARKS

An electroformed-nickel solar concentrator considered suitable for space-power use has been evaluated on a solar tracker with a water-cooled-cavity calorimeter used as the heat absorber. A concentrating efficiency of 0.75 was obtained at a concentration ratio (13,300) considered suitable for thermionic converter temperatures. Compensation of small errors in the lateral location of the calorimeter was obtained by adjustment of the angle between the optical axis and the solar rays.

Langley Research Center,
National Aeronautics and Space Administration,
Langley Station, Hampton, Va., June 28, 1965.

APPENDIX

CONVERSION OF U.S. CUSTOMARY UNITS TO SI UNITS

The International System of Units (SI) was adopted by the Eleventh General Conference on Weights and Measures, Paris, October 1960, in Resolution No. 12 (ref. 7). Conversion factors required for units used herein are:

Length: Inches × 0.0254 = meters (m)

Area: Square feet × 0.0929 = square meters (m^2)

Mass: Pounds × 453.59 = grams (g)

Temperature: 5/9 (^{o}Fahrenheit + 459.67) = ^{o}Kelvin (K)

Prefixes to indicate multiples of units are:

10^3 kilo (k)

10^{-2} centi (c)

REFERENCES

1. Sweetnam, G. E.: Power Sources. Supporting Research and Advanced Development. Space Programs Summary No. 37-19, Volume IV (Contract No. NAS 7-100), Jet Propulsion Lab., C.I.T., Feb. 28, 1963, pp. 47-55.

2. Smith, Arvin H.: A 500-Electrical-Watt Solar Energy Thermionic Conversion System for a Mars Spacecraft. Tech. Rept. No. 32-171 (Contract No. NAS 7-100), Jet Propulsion Lab., C.I.T., Apr. 15, 1962.

3. Von Doenhoff, Albert E.; and Hallissy, Joseph M., Jr.: Systems Using Solar Energy for Auxiliary Vehicle Power. Rept. No. 59-40, Inst. Aero. Sci., Jan. 1959.

4. Dawson, John R., and Heath, Atwood R., Jr.: Space-Station Power Systems. A Report on the Research and Technological Problems of Manned Rotating Spacecraft. NASA TN D-1504, 1962, pp. 59-70.

5. Heath, Atwood R., Jr.; and Maxwell, Preston T.: Solar Collector Development. Astronaut. Aerospace Eng., vol. 1, no. 4, May 1963, pp. 58-61.

6. Wilson, Volney C.; and Hamilton, Robert C.: Thermionic Convertors for Space Power. Astronaut. Aerospace Eng., vol. 1, no. 4, May 1963, pp. 62-67.

7. Mechtly, E. A.: The International System of Units. Physical Constants and Conversion Factors. NASA SP-7012, 1964.

8. Pichel, M. A.: Research and Development Techniques for Fabrication of Solar Concentrators. Rept. 1587-Final (Contract NAS 7-10), Electro-Optical Systems, Inc., Dec. 27, 1961.

9. Menetrey, W. R.: Solar Energy Thermionic Conversion System. Rept. No. 1850-Final (Contract No. JPL-950109), Electro-Optical Systems, Inc., Jan. 15, 1962.

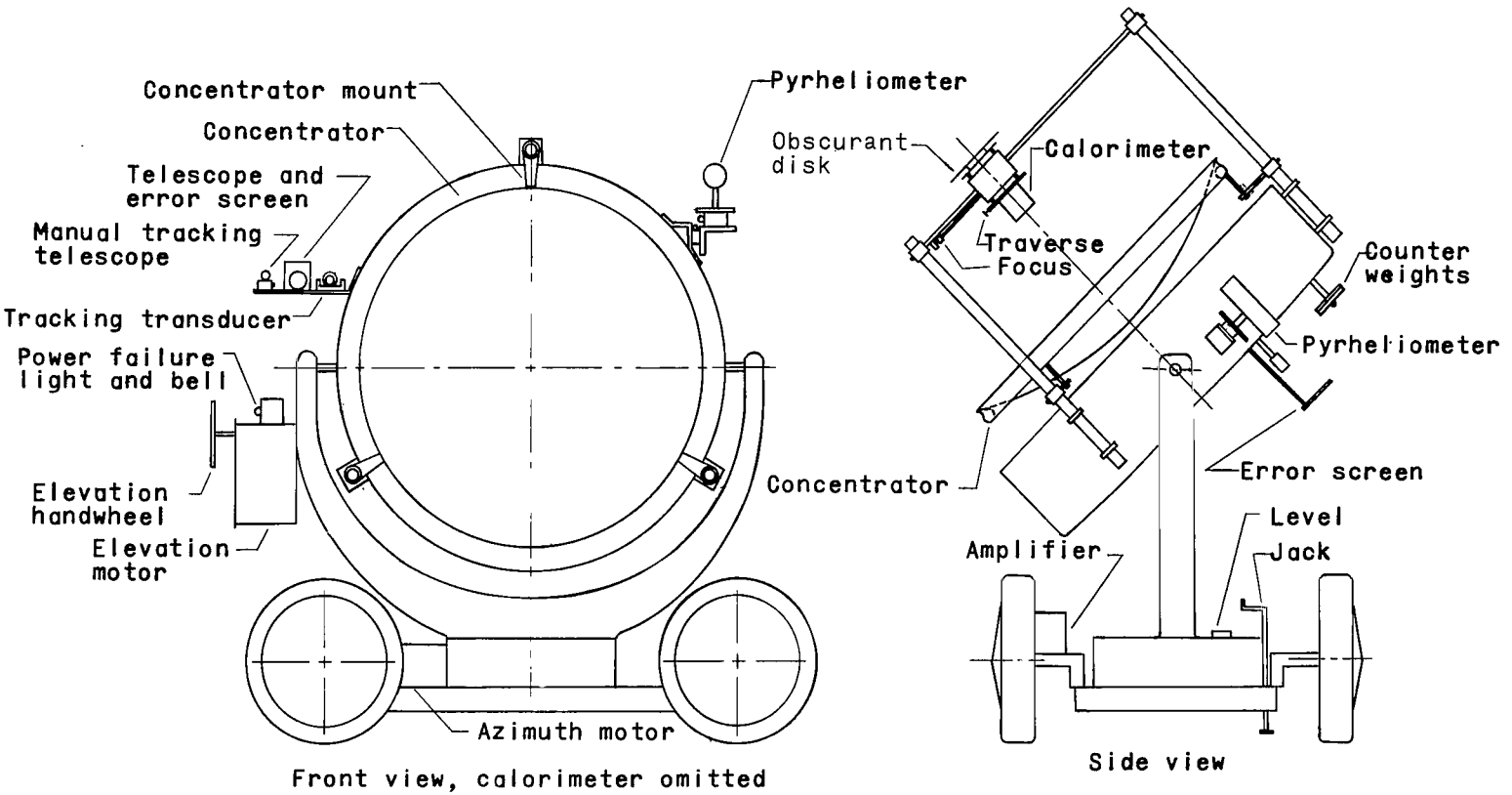

Figure 1.- Schematic of solar tracker.

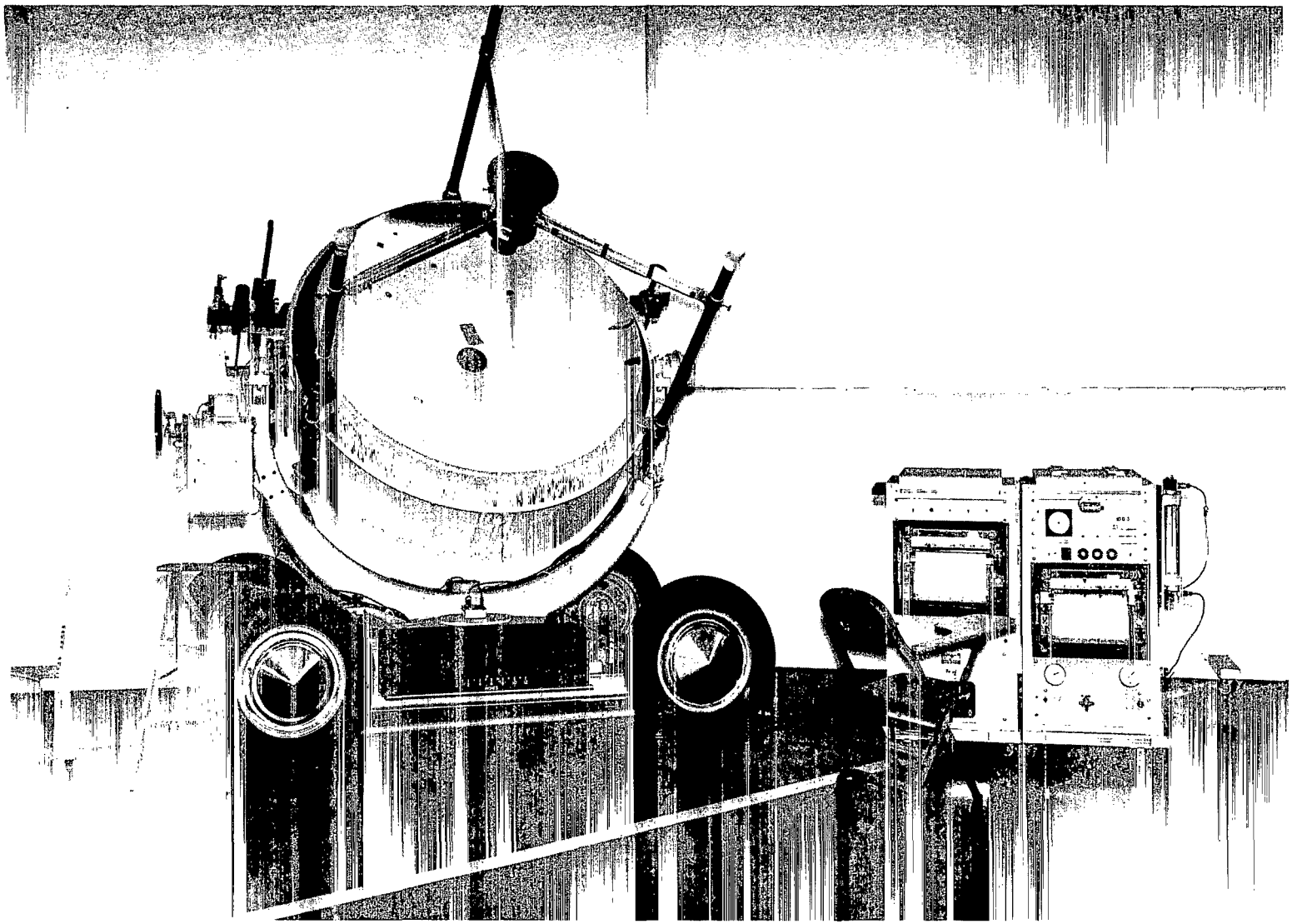

Figure 2.- Photograph of solar tracker and associated equipment. L-64-10,858

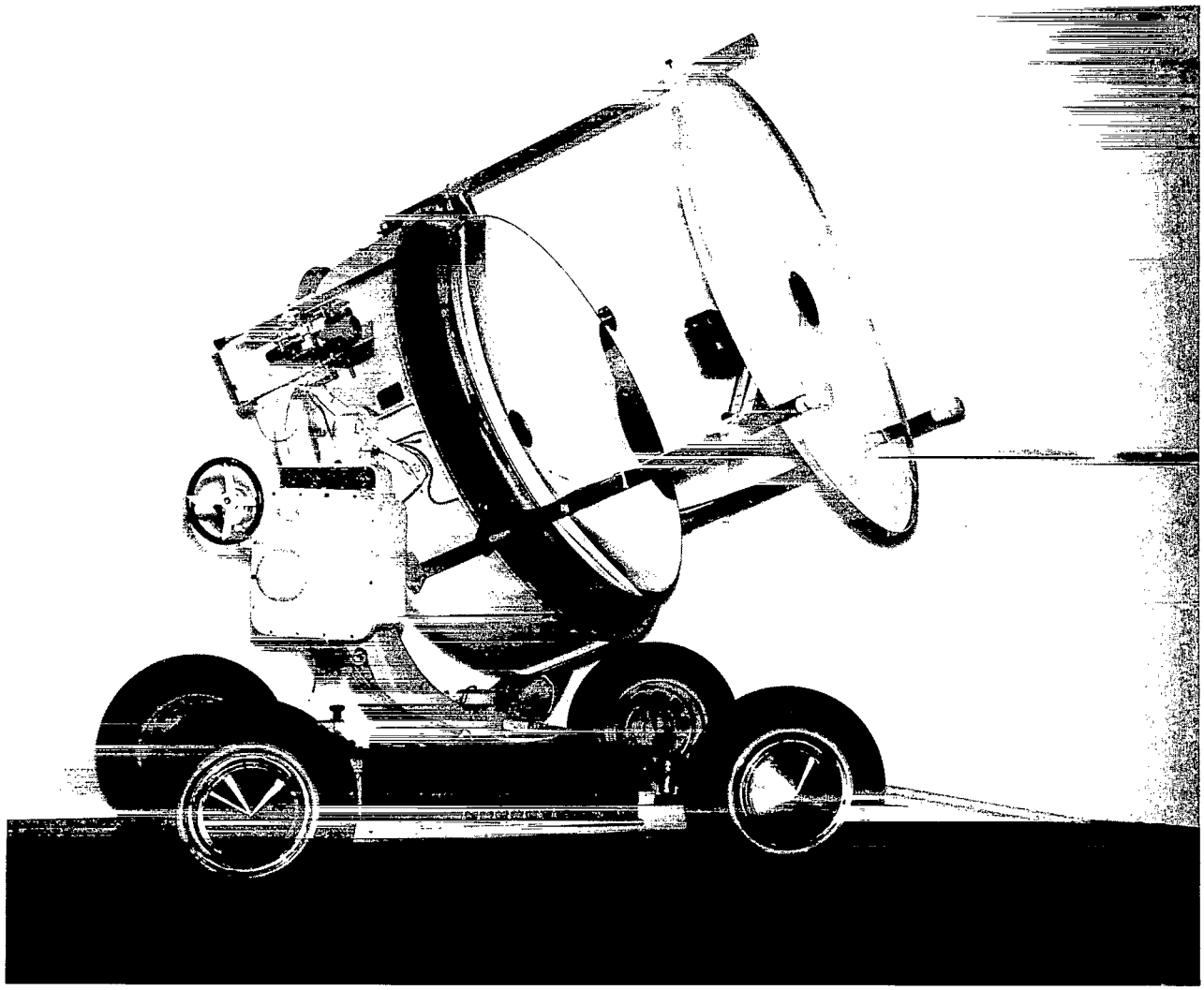

Figure 3.- Photograph of solar tracker with discrete Hartmann screen. L-64-10,859

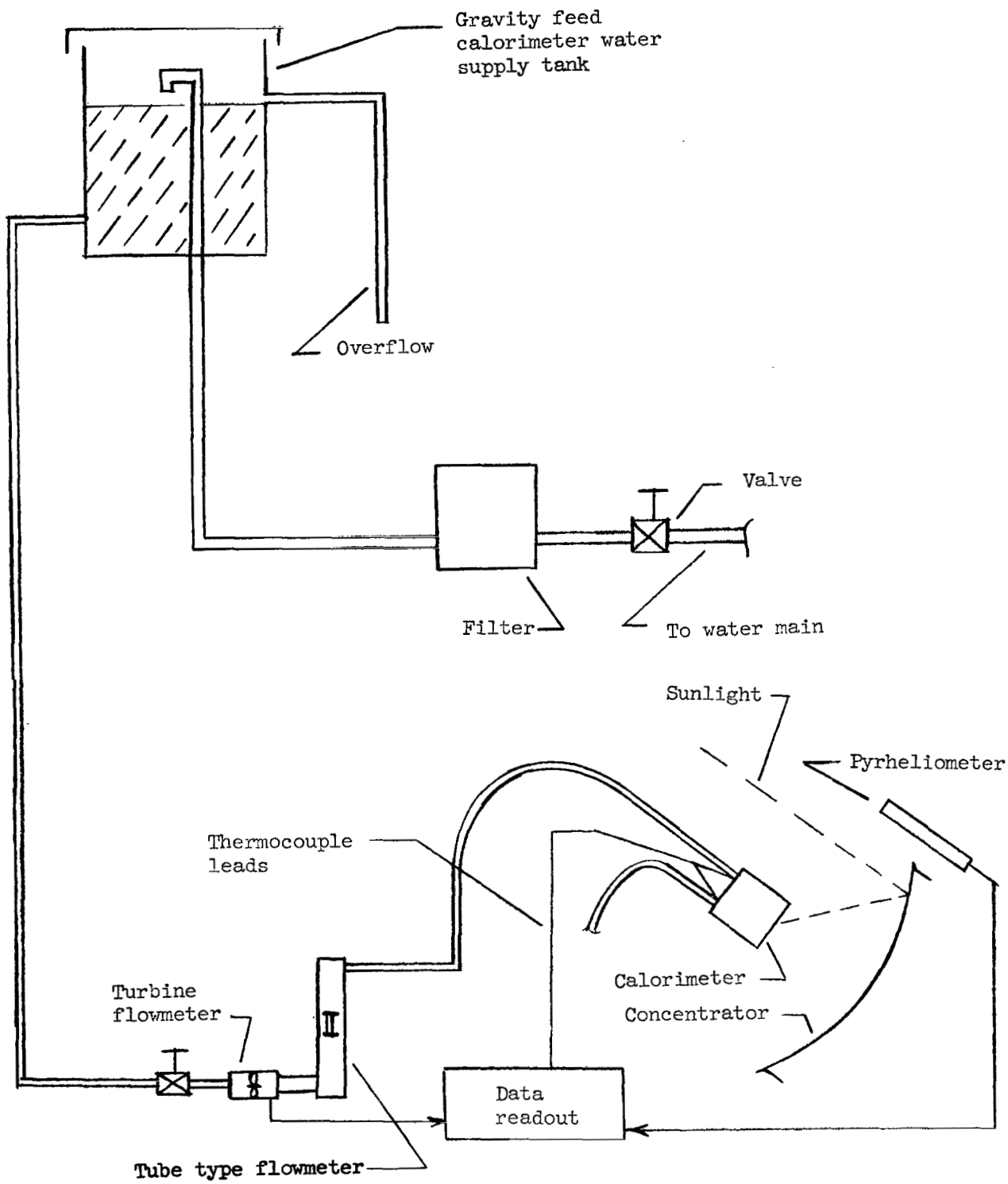

Figure 4.- Schematic of test facility.

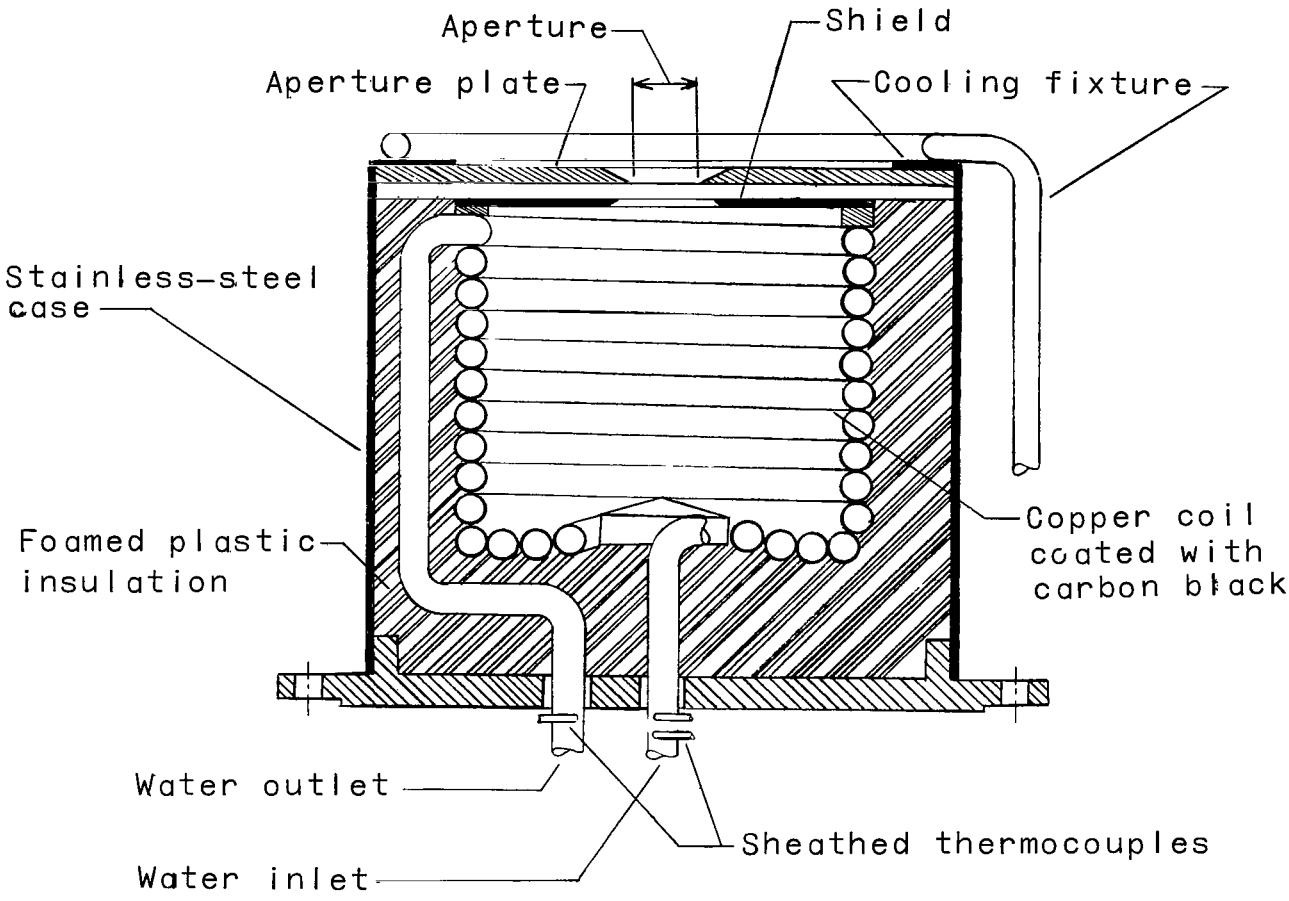

Figure 5.- Calorimeter.

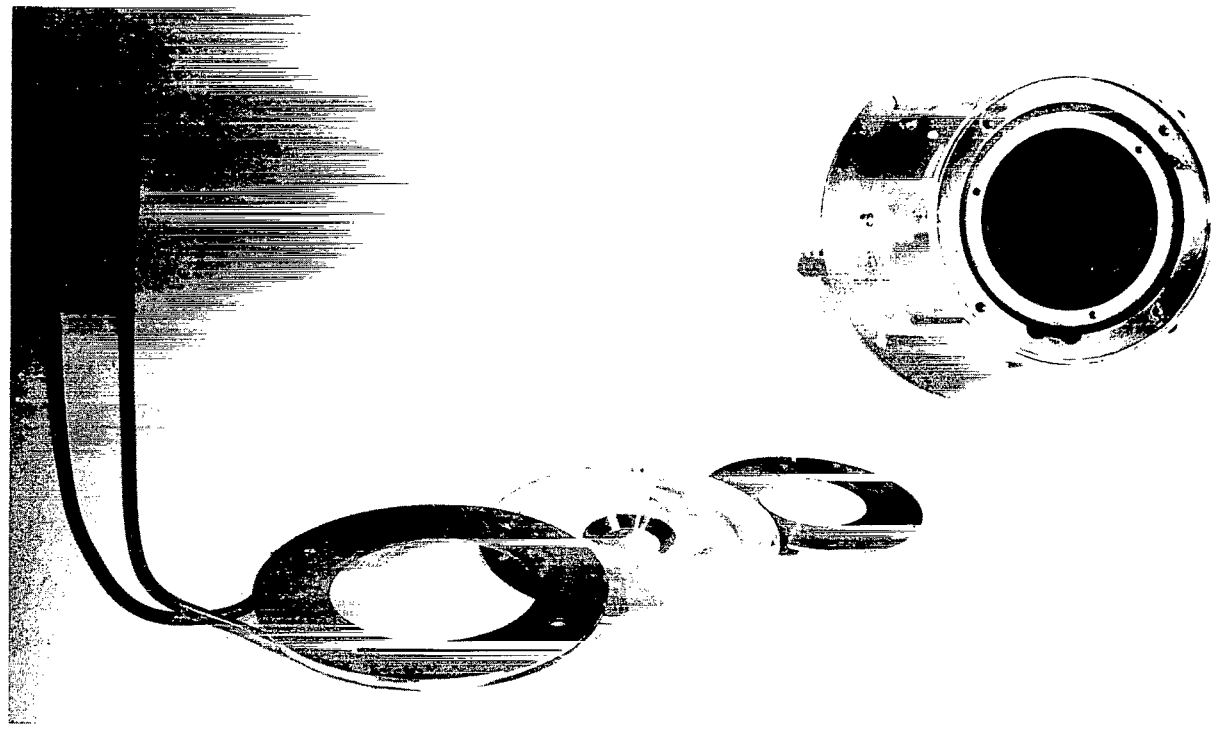

(a) Cooling fixture, aperture, and shield removed. L-63-9686

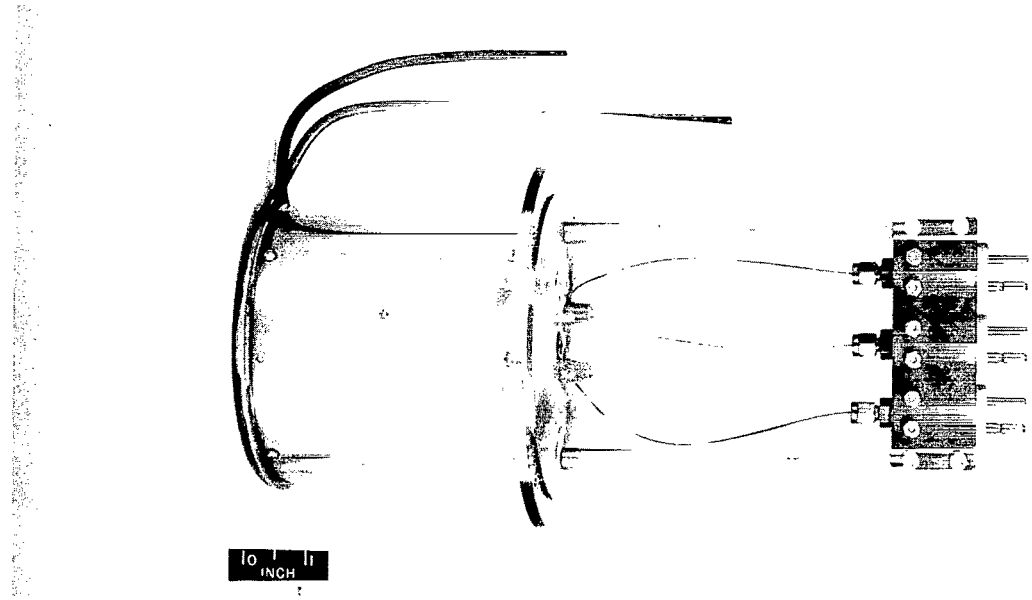

(b) Assembled. L-63-9687

Figure 6.- Photograph of calorimeter.

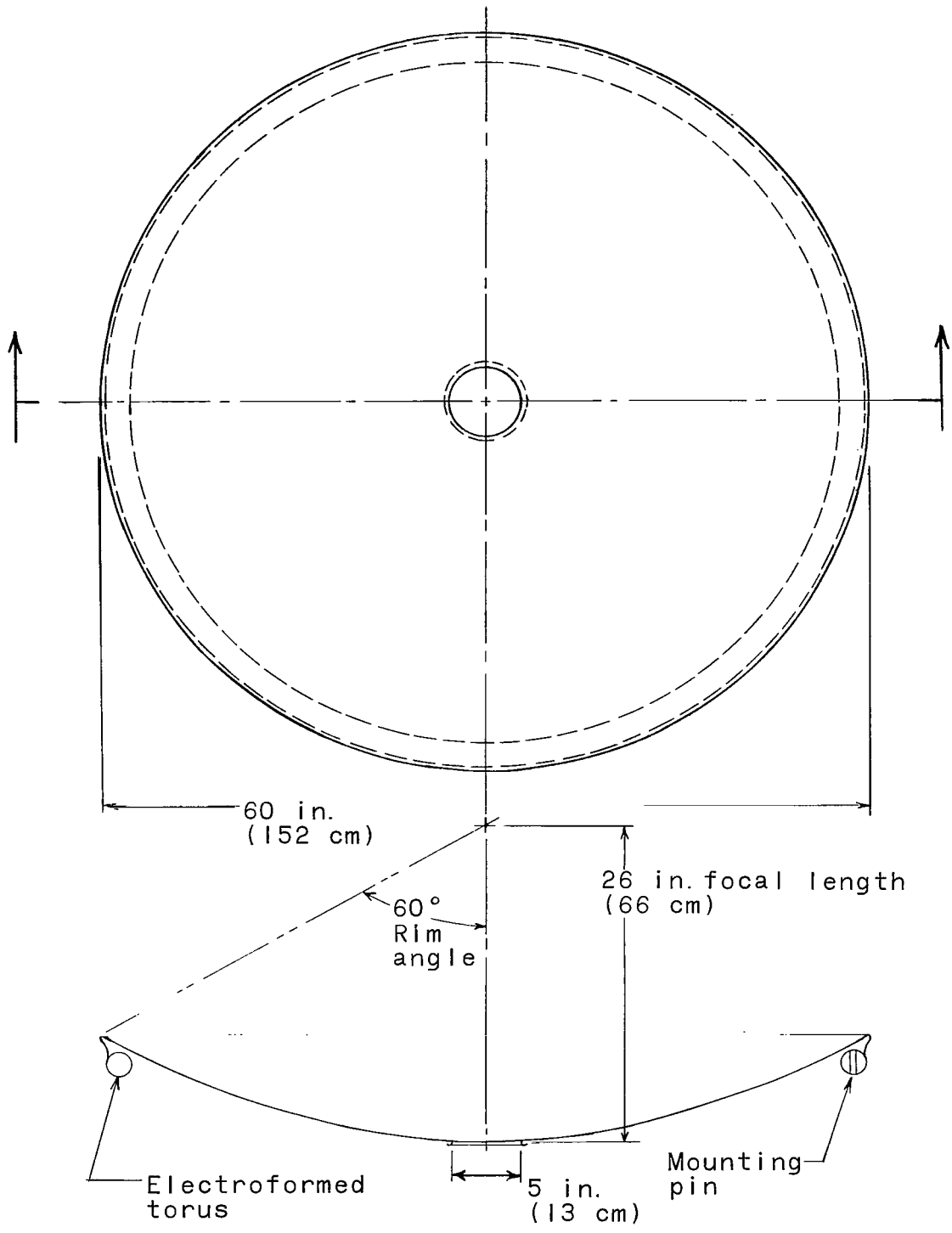

One piece electroformed nickel with a reflective coating of aluminum, no protective overcoat. 17.5 lbm (7.95 kg) mass.

Figure 7.- Concentrator geometry and construction.

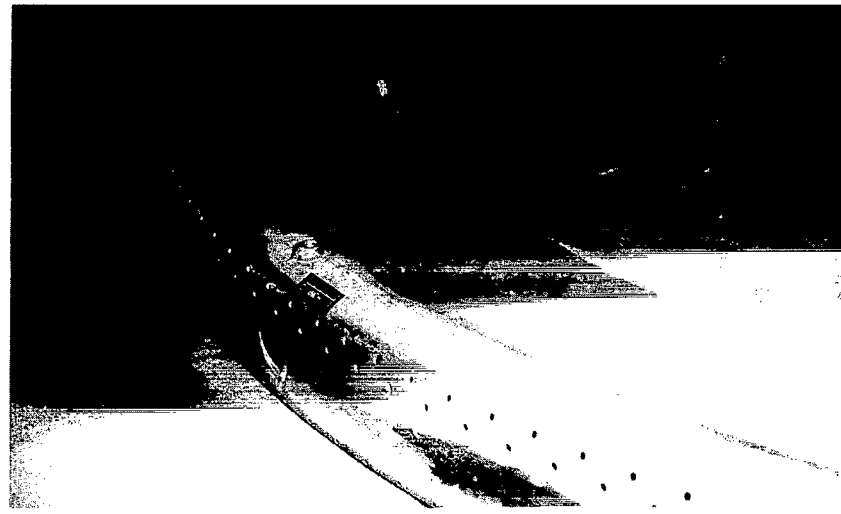

(a) Rear view of concentrator and support torus. L-64-10,861

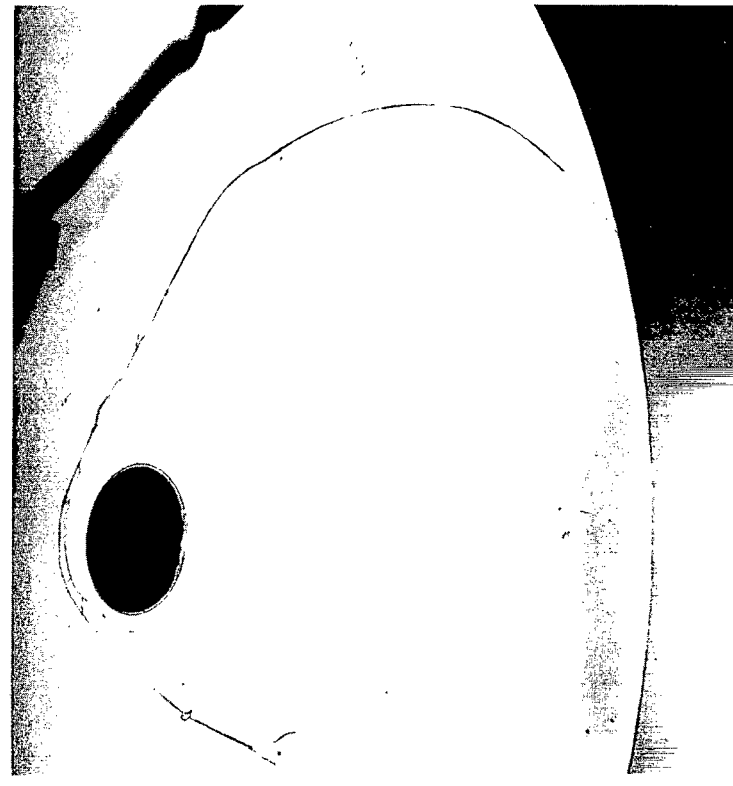

(b) Reproduction of crack which existed in master. L-64-10,860

Figure 8.- Photographs of concentrator.

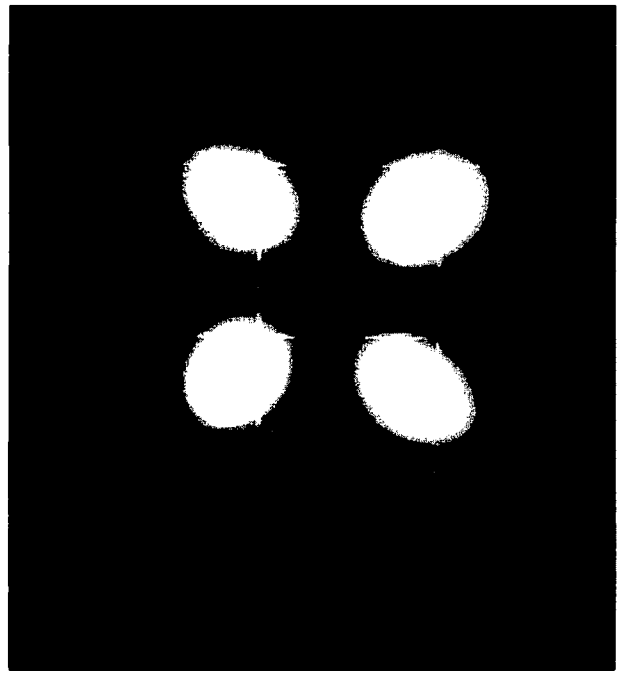

L-63-9525

Figure 9.- Photograph of typical images formed by using the discrete Hartmann screen.

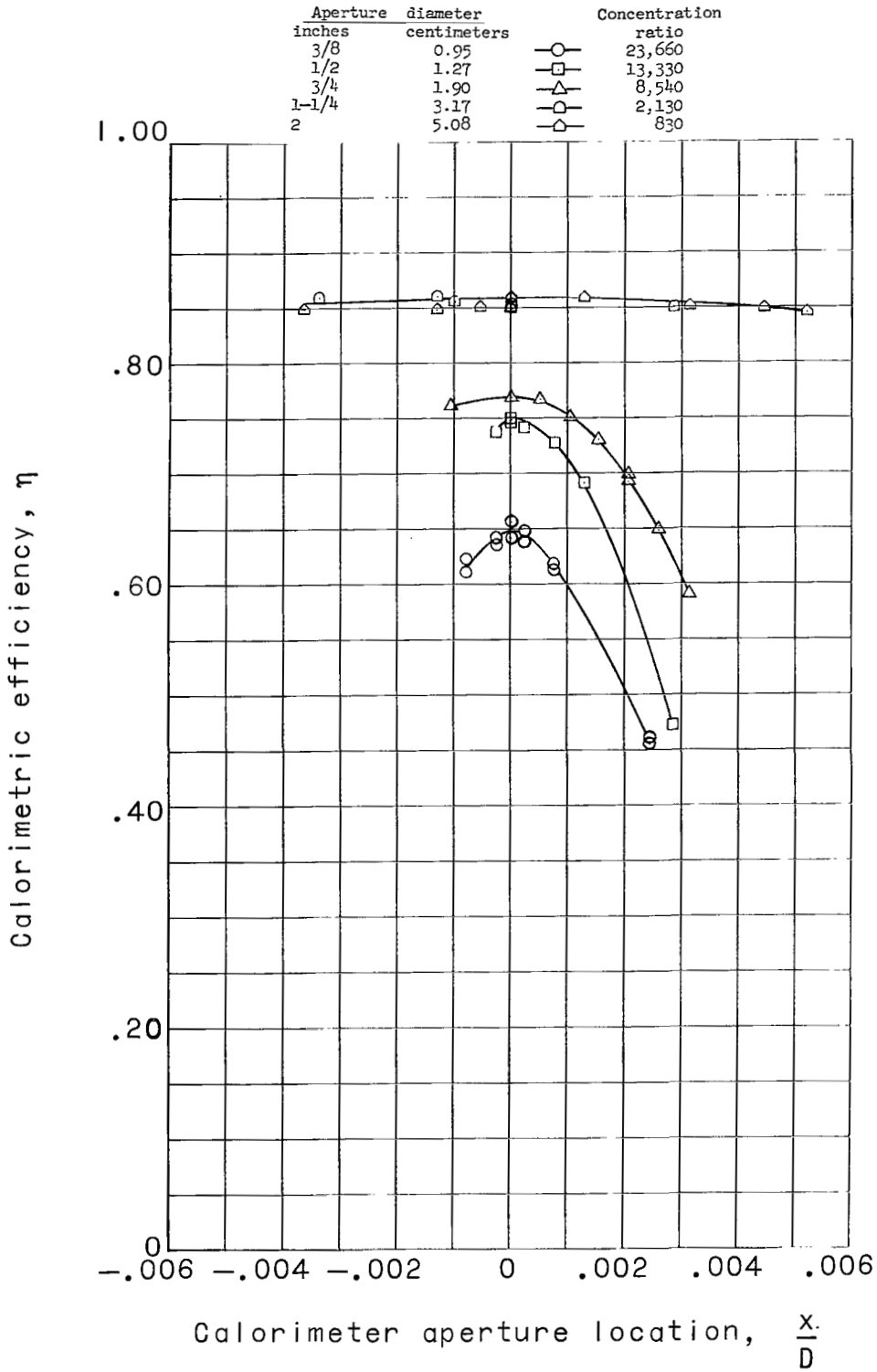

Figure 10.- Variation in concentrator efficiency with lateral location of calorimeter.

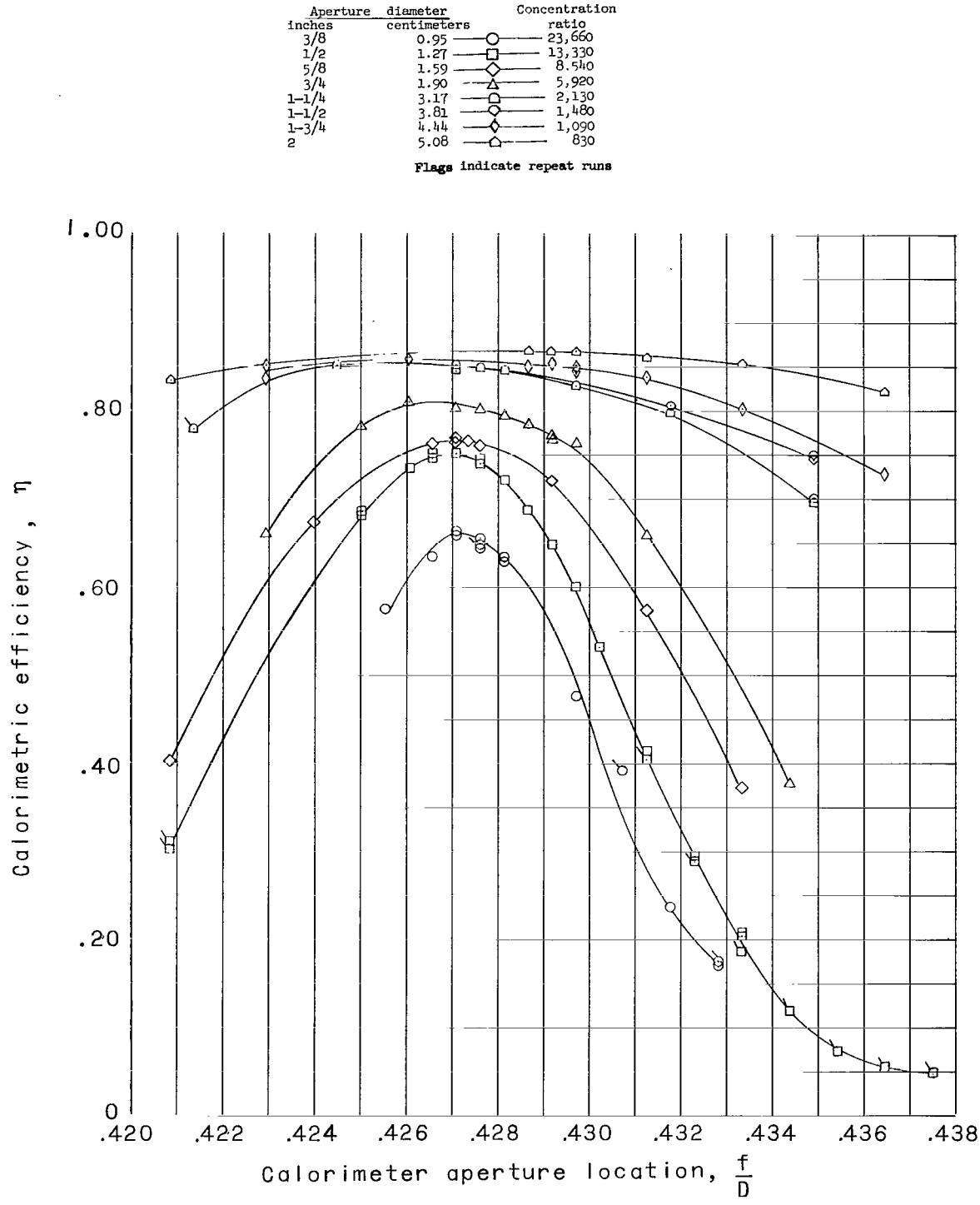

Figure 11.- Variation in concentrator efficiency with axial location of calorimeter.

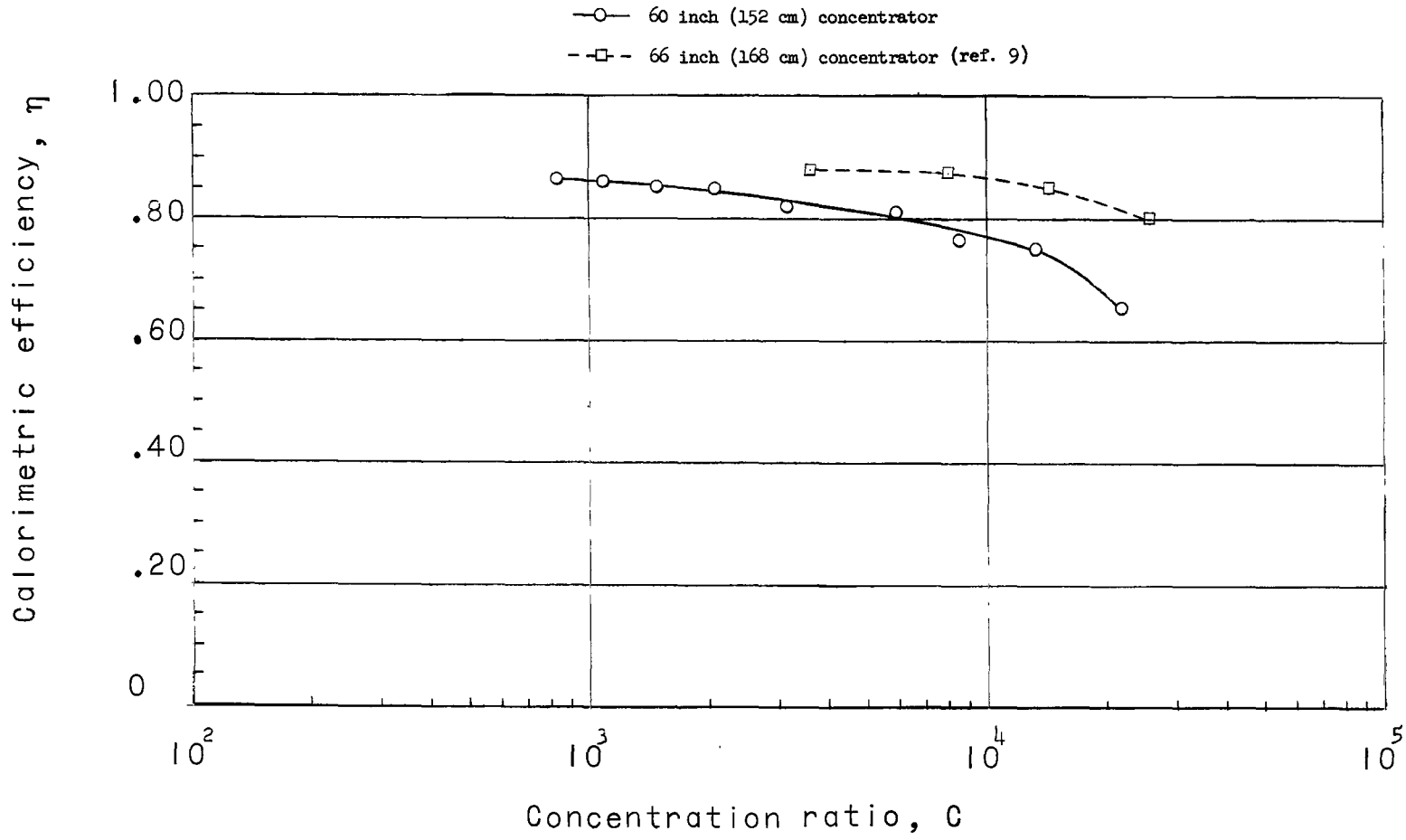

Figure 12.- Concentrator efficiency over a range of concentration ratios.

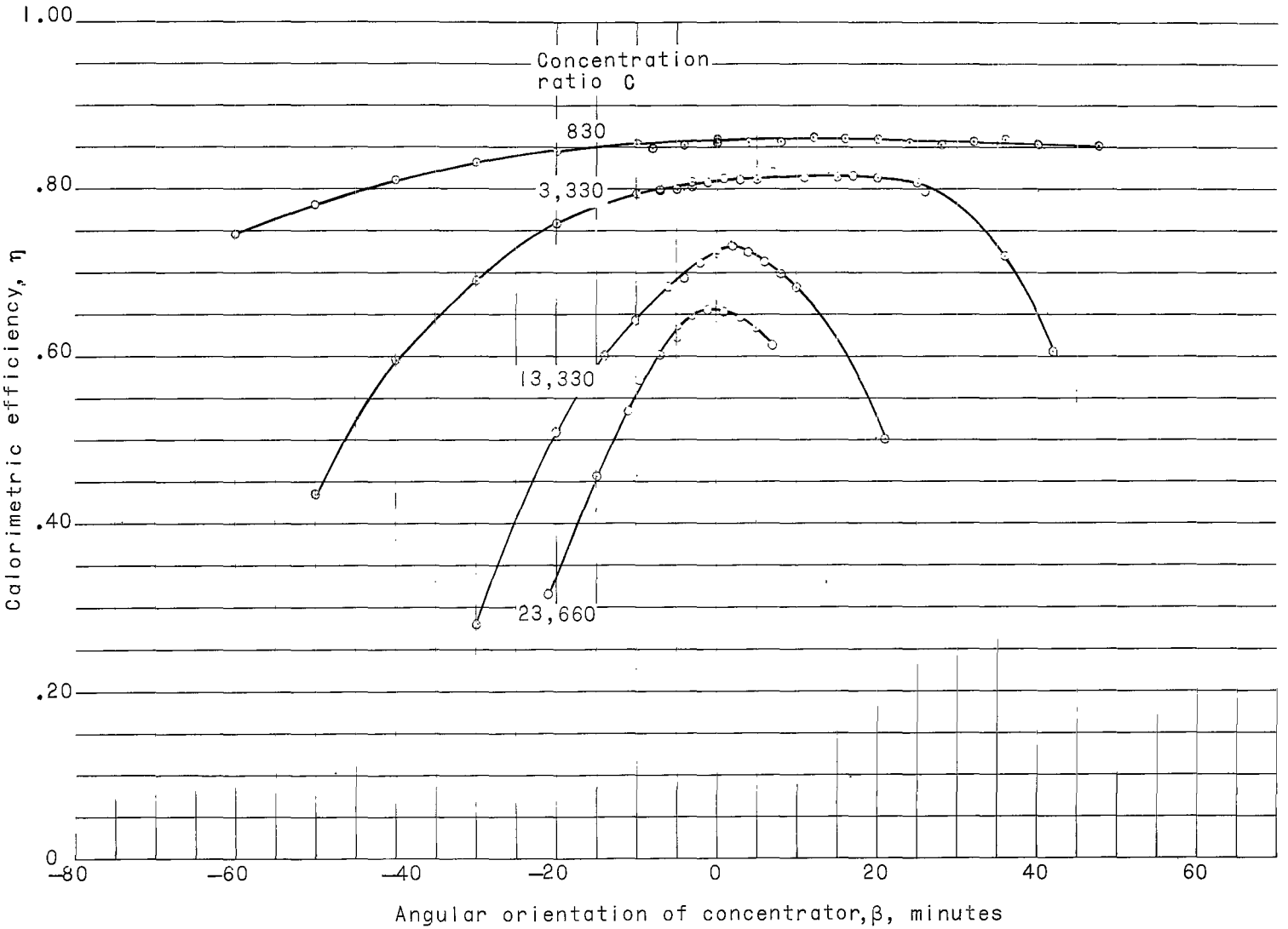

Figure 13.- Variations in concentrator efficiency due to angular orientation of concentrator-calorimeter system with respect to sun.

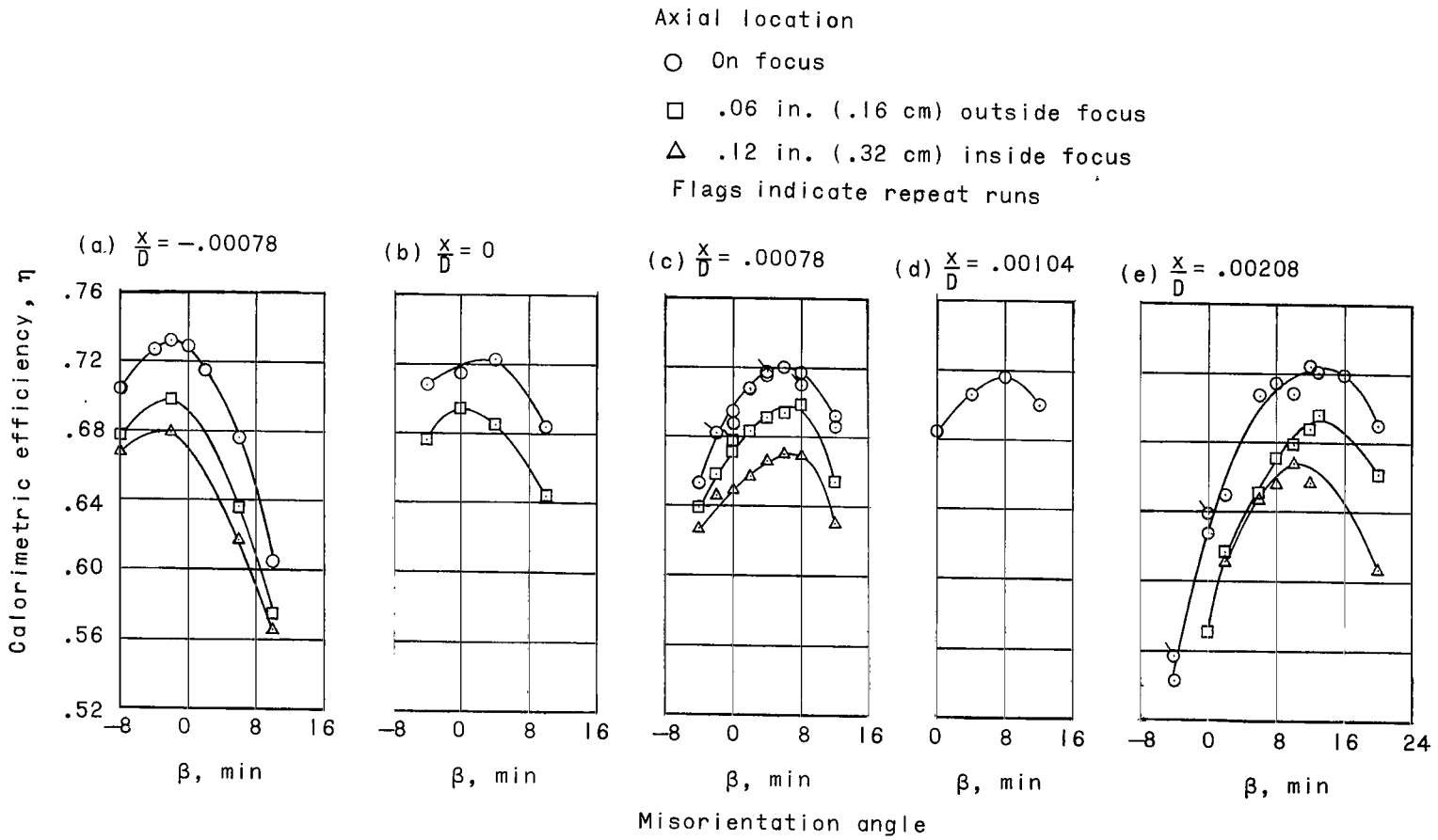

Figure 14.- Concentrator efficiency with combined variation in calorimeter location and concentrator orientation. C = 13,300.

"The aeronautical and space activities of the United States shall be conducted so as to contribute . . . to the expansion of human knowledge of phenomena in the atmosphere and space. The Administration shall provide for the widest practicable and appropriate dissemination of information concerning its activities and the results thereof."

—NATIONAL AERONAUTICS AND SPACE ACT OF 1958

NASA SCIENTIFIC AND TECHNICAL PUBLICATIONS

TECHNICAL REPORTS: Scientific and technical information considered important, complete, and a lasting contribution to existing knowledge.

TECHNICAL NOTES: Information less broad in scope but nevertheless of importance as a contribution to existing knowledge.

TECHNICAL MEMORANDUMS: Information receiving limited distribution because of preliminary data, security classification, or other reasons.

CONTRACTOR REPORTS: Technical information generated in connection with a NASA contract or grant and released under NASA auspices.

TECHNICAL TRANSLATIONS: Information published in a foreign language considered to merit NASA distribution in English.

TECHNICAL REPRINTS: Information derived from NASA activities and initially published in the form of journal articles.

SPECIAL PUBLICATIONS: Information derived from or of value to NASA activities but not necessarily reporting the results of individual NASA-programmed scientific efforts. Publications include conference proceedings, monographs, data compilations, handbooks, sourcebooks, and special bibliographies.

Details on the availability of these publications may be obtained from:

SCIENTIFIC AND TECHNICAL INFORMATION DIVISION

NATIONAL AERONAUTICS AND SPACE ADMINISTRATION

Washington, D.C. 20546